INSTITUTE OF PHYSICS PUBLISHING JOURNAL OF PHYSICS D: APPLIED PHYSICS

J. Phys. D: Appl. Phys. **38** (2005) 2625–2632 doi:10.1088/0022-3727/38/15/014

Imaging of *Caenorhabditis elegans* samples and sub-cellular localization of new generation photosensitizers for photodynamic therapy, using non-linear microscopy

G Filippidis[1], C Kouloumentas[1], D Kapsokalyvas[1], G Voglis[2], N Tavernarakis[2] and T G Papazoglou[1]

[1] Institute of Electronic Structure and Laser, Foundation of Research and Technology-Hellas, PO Box 1527, 71110 Heraklion, Greece

[2] Institute of Molecular Biology and Biotechnology, Foundation of Research and Technology, Heraklion 71110, Crete, Greece

E-mail: filip@iesl.forth.gr

Received 3 August 2004, in final form 22 November 2004
Published 22 July 2005
Online at stacks.iop.org/JPhysD/38/2625

Abstract

Two-photon excitation fluorescence (TPEF) and second-harmonic generation (SHG) are relatively new promising tools for the imaging and mapping of biological structures and processes at the microscopic level. The combination of the two image-contrast modes in a single instrument can provide unique and complementary information concerning the structure and the function of tissues and individual cells. The extended application of this novel, innovative technique by the biological community is limited due to the high price of commercial multiphoton microscopes. In this study, a compact, inexpensive and reliable setup utilizing femtosecond pulses for excitation was developed for the TPEF and SHG imaging of biological samples. Specific cell types of the nematode *Caenorhabditis elegans* were imaged. Detection of the endogenous structural proteins of the worm, which are responsible for observation of SHG signals, was achieved. Additionally, the binding of different photosensitizers in the HL-60 cell line was investigated, using non-linear microscopy. The sub-cellular localization of photosensitizers of a new generation, very promising for photodynamic therapy (PDT), (*Hypericum perforatum* L. extracts) was achieved. The sub-cellular localization of these novel photosensitizers was linked with their photodynamic action during PDT, and the possible mechanisms for cell killing have been elucidated.

(Some figures in this article are in colour only in the electronic version)

1. Introduction

The constant evolution of optical microscopy over the past century has been driven by the desire to improve the spatial resolution and image contrast with the goal of achieving a better characterization of smaller specimens. Numerous techniques such as confocal [1, 2], dark-field, phase-contrast, Brewster angle and polarization microscopies have emerged as improvements of conventional optical microscopy. Being a pure imaging tool, conventional optical microscopy suffers from its low physical and chemical specificity. This can be remedied by combining it with spectroscopic techniques

like fluorescence or Raman spectroscopy. In biology, such microscopes have been successfully applied to the study of a wide range of complex biological systems, with good spectral resolution. However their spatial resolution is restricted by the diffraction limit imposed by the wavelength of the probe light. Conventional microscopy also does not provide microscopic information about the real surface structure of the sample. Furthermore, it is insensitive to the polar organization of molecules in the surface layer, although this could be important.

In this context, non-linear optical measurements used in conjunction with microscopic observation have created new opportunities. Second-order non-linear processes such as second-harmonic generation (SHG) or sum frequency generation (SFG), and third-order processes such as third-harmonic generation (THG), coherent anti-Stokes Raman scattering (CARS) and two-photon excited fluorescence (TPEF) have been used for the imaging and understanding of biological systems and processes. In our work images and results obtained using the non-linear processes of the TPEF and SHG will be presented.

By far the most well known form of non-linear microscopy is based on TPEF. It is a three-dimensional imaging technology, an alternative to conventional confocal microscopy. It was firstly introduced by Denk *et al* [3] in 1990 and since then has become a laboratory standard. The electronic transition of a fluorophore can be induced by the simultaneous absorption of two photons. These two photons, typically in the infrared spectral range, have energies approximately equal to half of the energetic difference between the ground and excited electronic states. Since the two-photon excitation probability is significantly less than the one-photon probability, two-photon excitation occurs with appreciable rates only in regions of high temporal and spatial photon concentration. The high spatial concentration of photons can be achieved by focusing the laser beam with a high numerical aperture (NA) objective lens to a diffraction-limited focus. The high temporal concentration of photons is made possible by the availability of high peak power pulsing lasers, with pulse width of the order of hundreds of femtoseconds (10^{-15} s). The most important feature of two-photon microscopy is its intrinsic depth discrimination. This depth discrimination effect of the two-photon excitation arises from the quadratic dependence of two-photon fluorescence upon the excitation photon flux, which decreases rapidly away from the focal plane. The ability to limit the region of excitation is very important, especially for biological specimens, since their photodamage is restricted only to the focal point. Since out-of-plane fluorophores are not excited, they are not subject to photobleaching. Moreover, TPEF microscopy exhibits an additional advantage. Two-photon excitation wavelengths are red-shifted to approximately twice the one-photon excitation wavelengths. The significantly lower absorption and scattering coefficients ensure deeper tissue penetration.

A less known form of non-linear microscopy, SHG microscopy, was used several years prior to the use of TPEF, based on the generation of second-harmonic light either from surfaces or from endogenous tissue structures such as rat-tail tendons. In SHG, light of the fundamental frequency, ω, is converted by the non-linear material into light at exactly twice that frequency, 2ω. Because of difficulties in signal interpretation and because of its seemingly 'arcane' utility, at least in biological imaging, SHG microscopy has gone by relatively unnoticed until very recently. The discovery that exogenous markers can lead to exceptionally high signal levels has been a leading cause for the revival of SHG microscopy. In particular, SHG markers, when properly designed and collectively organized, can produce signal levels easily comparable with those encountered in standard TPEF microscopy. Apart from that, many intrinsic structures of biological systems produce a strong SHG signal, and so labelling with exogenous molecular probes is not always required. The spatial resolutions provided by SHG and TPEF microscopies are commensurate, meaning that the two contrast modes can be conveniently derived from the same setup. Despite their similarities, TPEF and SHG are based on fundamentally different phenomena [4]. TPEF relies on non-linear absorption, followed by fluorescence emission and hence is not a coherent process. SHG, on the other hand, relies on non-linear scattering and hence is a coherent process. SHG, like TPEF, exhibits intrinsic three-dimensionality and ability to section deep within a biological tissue, due to its non-linear nature. It has a significant efficiency only at extremely high incident light intensities, and therefore emanates only from a well-defined volume around the focal centre of the incident light beam. Moreover, in the SHG imaging technique, like TPEF, the wavelength of the fundamental incident light lies in the IR spectrum region, thus suffering less from scattering and absorption inside biological samples and exhibiting large penetration depths. We have already mentioned that an enabling aspect of TPEF microscopy is the dramatic reduction of 'out of focal plane' photobleaching and phototoxicity, compared with conventional fluorescence microscopy. However, these effects still occur 'in the plane' of focus. By contrast, in SHG microscopy, photodamage considerations do not intrinsically exist, since as was mentioned, SHG does not arise from an absorptive process. However, photobleaching usually accompanies SHG if the incident beam produces simultaneously two-photon excitation of the chromophores in the sample. Due to their similarities and their differences, TPEF and SHG can be combined in a single microscope, and this combination can be very advantageous, since they provide complementary information about several biological systems [5–8].

SHG is a second-order non-linear phenomenon, and its strength is fully determined by the second-order susceptibility tensor, $\chi^{(2)}$, of the non-linear medium. This tensor is non-vanishing only for non-centrosymmetric media. Under this symmetry constraint it is obvious that SHG can be mainly produced from structures with a high degree of orientation and organization but without inversion symmetry, such as crystals or endogenous arrays of structural proteins in biological systems. It can be also produced from metal surfaces, where there is a huge change in the refractive indices, and generally from interfaces, where the symmetry breaks. Over the last two decades SHG has been widely used as a spectroscopic tool in a variety of interfacial studies, including liquid–solid, liquid–air and liquid–liquid interfaces [9]. Because of the interfacial specificity of the process, SHG is an ideal

approach to the study of biophysics in model membranes [10, 11], the membrane physiology of living cells [12–14] and endogenous structural proteins [15–17]. Particularly, one of the innovative applications of the SHG phenomenon is its usage as a highly sensitive monitor of membrane potential [18–22].

In this work, we present detailed imaging of the nematode *Caenorhabditis elegans* using non-linear microscopy. Wild type worms and transgenic animals which express the green fluorescence protein (GFP) in the pharyngeal muscle cells have been imaged. Additionally, in order to explore the fermentations that govern photodynamic therapy (PDT), TPEF images from leukemic cells (HL-60) embedded with photosensitizers were obtained. We used merocyanine 540 (MC-540) and *Hypericum perforatum* L. extracts as photosensitizers.

2. Experimental apparatus

The development of a reliable, flexible, compact, inexpensive experimental apparatus for recording two-photon and SHG images at the microscopic level constitutes the initial target of this study. A proper modified, common, inexpensive microscope was used. A low cost motorized x–y–z translation stage was used for the scanning procedure. Since the commercial two-photon microscopes and the laser scanning devices are very expensive, the development of a reliable, low-cost setup for real-time non-linear measurements would be useful for a variety of experiments in the field of biology.

In figure 1 the layout of the developed setup for combined TPEF–SHG scanning microscopy is depicted, and its main parts are shown. We use as the excitation source a diode-pumped, femtosecond t-pulse laser (Amplitude Systemes product—high power femtosecond oscillator) emmited at 1028 nm. The laser material is an Ytterbium-doped crystal. The small size of the laser permits the whole setup to be extremely flexible. The average output power is 1 W, and it is characterized by long-term stability. The pulse duration is 200 fs and the repetition rate is 50 MHz. Using the above specifications, the energy of the single pulse is calculated to be 20 nJ. This amount of energy, limited in 200 fs, is extremely high and provides high efficiency of exciting non-linear phenomena. The beam is directed to a modified optical microscope (Nikon Eclipse ME600D) using suitable dichroic mirrors. The last dichroic mirror (99% reflectivity at 1000 nm) directs the fundamental beam to the objective lens. The objective lens offers the necessary tight focusing of the fundamental beam onto the sample. Simultaneously, it collects the TPEF originating from the sample in the backward direction and collimates this signal, which is directed to the photomultiplier tube (PMT) at the top of the microscope. The average laser power on the specimen is 10 mW. The biological sample is mounted between two cyclic glass slides. The thickness of each glass slide is 50–70 μm. The need for a thin slide originates from the short working distance of the objective lens. The slides are positioned at a special holder. This holder is connected mechanically with the x–y–z scanning stage. The x–y–z motorized scanning stage is a combination of three 'one-dimensional' Standa 8MT167-100 step motors. Their minimum step is 1 μm, and this sets a limit in the transversal and in the longitudinal resolution potentials of our system. The combined movement of the three stages is computer controlled by our specially designed software (National Instruments, Labview program 6.1), so that a complicated scanning scheme is created. The average accumulation time in every step is 30 ms.

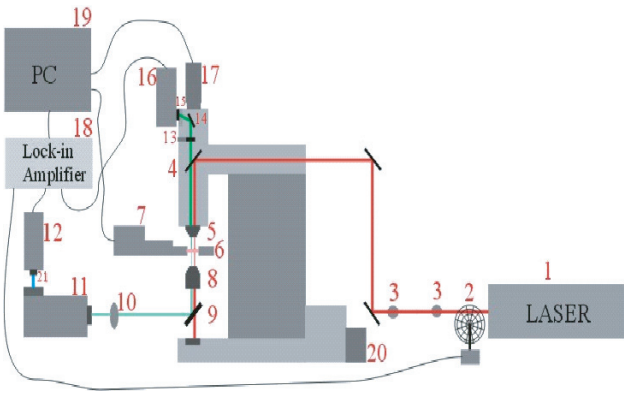

Figure 1. Experimental set-up for combined TPEF–SHG scanning microscopy: (1) femtosecond laser ($\lambda = 1028$ nm), (2) chopper, (3) iris, (4) dichroic mirror, (5) objective lens, (6) holder of the sample, (7) x–y–z motorized scanning stage, (8) condenser lens, (9) dichroic mirror, (10) focusing lens, (11) monochromator, (12) photomultiplier tube (PMT), (13) neutral density filter, (14) flip-mount mirror, (15) short-pass filter, (16) PMT, (17) CCD camera, (18) lock-in amplifier, (19) PC, (20) light source, (21) short-pass filter. The SHG signal is detected in the forward direction (PMT 12), while the TPEF is detected in the backward direction (PMT 16).

For thin samples (like in our case) almost the entire signal of the SHG propagates with the laser and is collected and collimated by the condenser lens of the microscope (NA 0.9, working distance 1.9 mm). A dichroic mirror is positioned under the condenser (99% at 45°, 450–650 nm). TPEF and SHG signals are focused by means of a lens into the slit (100 μm) of a monochromator. This is important for proper operation of the monochromator, and prevents loss of the signal. The focal length of the lens is 3 cm. The monochromator (Digikrom CM110 CVI) consists of a grating (600 grooves mm^{-1}) adequate for visible light. For detection of the signals a photomultiplier tube (PMT Hamamatsu R636-10) is used. A short-pass filter (SPF 700 nm CVI) is placed before the PMT in the forward direction in order to cut off the remainder of the laser light. The PMT is connected to the lock-in amplifier (SR810 Stanford Research Systems), where the created current is converted to a voltage indication. By using this configuration it is feasible to collect both SHG and TPEF signals in distinct sets of measurements (by tuning the monochromator to the proper wavelength).

Furthermore, TPEF signals are collected using a photomultiplier tube (PMT Hamamatsu R4220) that is attached at the position of the eye-piece of the microscope. The PMT is also connected to the lock-in amplifier. A short-pass filter (SPF 650 nm CVI) is placed before the PMT at the top of the microscope in order to cut off the reflected laser light. For optical observation of the biological samples through the objective lens, a CCD camera (Sony XC-57CE) is employed.

By using the whole experimental apparatus it is possible to collect SHG and TPEF signals simultaneously (by detecting

SHG images in the forward direction and TPEF images in the backward direction). Matlab 6.0 (the MathWorks Inc.) was used for processing of the obtained three-dimensional data.

3. Biological samples

3.1. Caenorhabditis elegans

C. elegans is a small (1 mm) free-living hermaphroditic nematode that completes a life cycle in 2.5 days at 25°C. The simple body plan and transparent nature of both the egg and the cuticle of this nematode have facilitated an exceptionally detailed developmental characterization of the animal. The complete sequence of cell divisions and the normal pattern of programmed cell deaths that occur as the fertilized egg develops into the 959-celled adult are known [23]. One considerable advantage of the *C. elegans* system is that it is the first metazoan for which the genome was sequenced to completion [24]. Another advantage of this system is that construction of transgenic animals is rapid; DNA injected into the hermaphrodite gonad concatamerizes and is packaged into embryos in the form of an extra chromosomal array, hundreds of which can be obtained within a few days of the injection [25]. The anatomical characterization and understanding of neuronal connectivity in *C. elegans* are unparalleled in the metazoan world. Serial section electron microscopy has identified the pattern of synaptic connections made by each of the 302 neurons of the animal (including 5000 chemical synapses, 600 gap junctions and 2000 neuromuscular junctions), so that the full 'wiring diagram' of the animal is known [26]. Overall, the broad ranges of genetic and molecular techniques applicable in the *C. elegans* model system allow a unique line of investigation into fundamental problems in biology.

We followed standard procedures for *C. elegans* strain maintenance, crosses and other genetic manipulations [27]. The nematode rearing temperature was kept at 20°C. Before each experiment, young adult animals were anaesthetized by immersing in 0.5 M of sodium azide (NaN_3), and subsequently they were mounted on glass slides.

3.2. Leukemic cell line HL-60

The HL-60 cell line (acute promyelocytic leukemia) was used and maintained in RPMI-1640 with 10% foetal calf serum (FCS), 1% penicillin–streptomycin, 1% L-glutamine and 1% sodium pyruvate at 37°C in a humidified atmosphere of 5% CO_2 in air. Cells were maintained in log phase with 95% viability.

Cells (HL-60) were adjusted at a concentration 3×10^6 ml^{-1} and incubated with the photosensitizer for 1 h at 37°C in a 5% CO_2 humidified atmosphere before the measurements.

3.2.1. Photosensitizers. (A) Merocyanine 540 (MC-540) was obtained from Sigma Chemical Co (St. Louis, USA). A stock solution of MC-540 was prepared in 50% ethanol–water at 1 mg : ml^{-1} and stored at 20°C in small aliquots. The concentration of MC-540 used to stain the cells was 20 μg ml^{-1}. This concentration of the photosensitizer was chosen since it yielded the optimum results in cancer cell killing during PDT [28].

(B) *Hypericum perforatum* L. extracts come from the dry herb. Extraction of dry herb with methanol yields the methanolic extract (ME) at 11% concentration, which is then fractionated using liquid/liquid extraction, yielding the polar methanolic fraction (PMF) in 10% overall yield. Hypericin, a photosensitizing ingredient of the herb, was found in these extracts in concentrations as low as 0.51%, and 0.57%, respectively. The concentration of each extract (PMF or ME) used to stain the cells was 50 μg ml^{-1}. This concentration was chosen since it yields the optimum results, for both photosensitizers, in HL-60 cell killing during PDT (unpublished data).

4. Results

For performing our measurements an inexpensive, reliable, flexible, compact experimental apparatus for imaging of biological samples by using non-linear microscopy was developed. The non-linear processes of SHG and TPEF were employed to obtain the images.

Our first objective was detailed imaging of various *C. elegans* cell types and determination of the endogenous structural proteins of the worm that produce SHG signals effectively. Figure 2 shows an SHG image of the anterior part of *C. elegans*. In the strain we used in this experiment the GFP molecules are expressed under the control of the *myo-2* promoter. This promoter is tissue-specific and the GFP expression is limited to the cytoplasm of the pharyngeal muscle cells. The signal was recorded in the forward direction. The monochromator was tuned at 514 nm. Therefore, the SHG is the dominant factor in the collected signals. The spectral distribution of the recorded signal has the characteristics of SHG with the FWHM being ~4 nm (FWHM of the fundamental laser beam ~6 nm). Due to the excitation wavelength (1028 nm), at 514 nm the signal comprises both SHG and TPEF from GFP molecules. The independently measured SHG signal is at least 30 times stronger than the TPEF counterpart at 514 nm. Thus, the contribution of the latter can be considered insignificant and in any case does

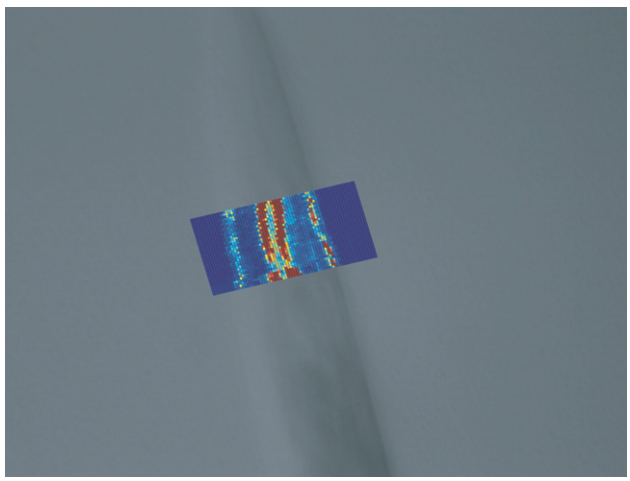

Figure 2. SHG imaging of *C. elegans*, which expresses GFP molecules in the pharyngeal muscle cells. The image was recorded from the anterior part of the worm. The pharynx and the edges of the nematode are outlined.

not affect essentially the SHG scanning image. The collected signal exclusively comes from TPEF from GFP molecules for $\lambda > 518$ nm.

For the experiments a Nikon (50×, NA 0.8) objective lens was used since the NA of the condenser lens (0.9) must be higher or equal compared with the objective lens in order to collect the whole cone of light. The scanning was performed in a specific z position where the recorded SHG signal arises from the sample was maximum. The dimensions of the scanned region are $34 \times 66\,\mu m^2$, with the minimum step being $1\,\mu$m in each direction. SHG imaging of the anterior part of the *C. elegans* nematode was possible due to the high signal levels from the muscles around the pharynx and the muscles of the body walls at the edges of the nematode. The endogenous structural protein that gives rise to the SHG signal is mainly actomyosin [14]. Actomyosin assemblies are the main components of the sarcomere, i.e. of the skeletal muscle. Their SHG efficiency is proved by our image, since the SHG signal is produced strongly from parts of the nematode where relatively thick muscles are located. Furthermore, collagen very likely participates in the outline of the nematode, since it is one of the basic ingredients of the hypodermis and has great SHG efficiency due to its highly crystalline, not centro-symmetric, triple-helix structure. Consequently, the actomyosin complexes and collagen are the main contributors to the recorded SHG signal from the anterior part of the worm. In order to determine the contribution of the randomly oriented GFP molecules to the recorded non-linear signal, SHG images from the pharynx of wild type *C. elegans* were obtained. Wild type worms are not genetically manipulated, and thus they do not express GFP in any part of their body. Figure 3 shows an endogenous SHG image from the anterior part of a wild type *C. elegans*. The dimensions of the scanned region are $60 \times 120\,\mu m^2$ with the minimum step being $2\,\mu$m in each direction. The sacromeres are seen in a large portion of the chewing mechanism. Additionally, the body wall muscles at the edges of the animal are detectable. Comparing figures 2 and 3, we come to the conclusion that the GFP molecules, due to their random orientation, do not possess SHG efficiency. The acquired SHG images and our findings from the pharynx of the *C. elegans* are in good agreement with the data from other very recent studies (Campagnola and Loew [14]). Furthermore, in our study the use of 1028 nm as the excitation source, instead of the typical wavelength around 800 nm, was chosen in order to further reduce photodamages of the biological specimens (due to the lower energy per photon).

In the second part of our study the sample under investigation was the HL-60 cell line. It is a promyelocytic cell line, derived from patients with acute promyelocytic leukemia. This study was performed in order to explore the fermentations that govern PDT and to increase its efficiency. The cells were stained with photosensitizers. Merocyanine 540 (MC-540) and *Hypericum perforatum* L. extracts were used as photosensitizers. The photosensitizer is bound to the membrane of the cancer cells, but in some cases it can penetrate into the intracellular domain. The localization of the different photosensitizers inside the cell by means of an imaging technique can provide useful information about their action and their effectivity. Moreover, it can be helpful in the design of more selective photosensitizers. In this line of investigation we used the developed non-linear microscope for localization of the photosensitizers in a specific cell line (HL-60) and we compared our results with the corresponding images obtained using a commercial one-photon confocal fluorescence microscope.

We performed TPEF scanning imaging in cells stained with merocyanine 540 (figure 4). For these experiments a Nikon (50×, NA 0.8) objective lens was used, and the TPEF signal was detected in the backward direction. The scanning was performed in a specific z position where the recorded TPEF signal emanating from the sample was maximum. The dimensions of the scanned region are $30 \times 25\,\mu m^2$, with the minimum step being $1\,\mu$m in each direction. Examining figure 4, we note that the merocyanine 540 does not remain strictly membrane bound and it has the potential to penetrate into the intracellular domain of the cell [29]. Comparative imaging using the one-photon confocal

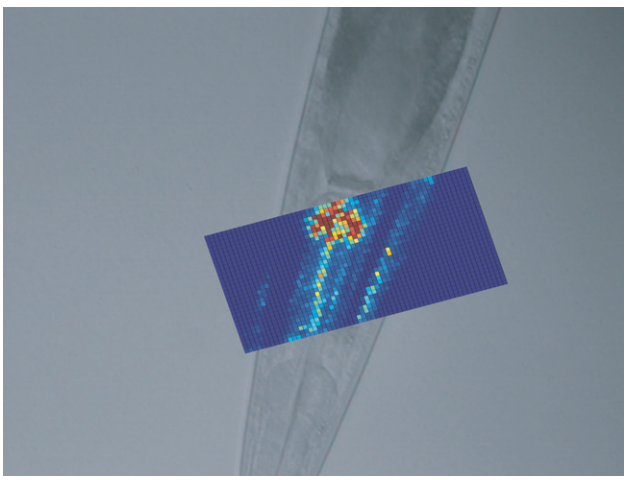

Figure 3. Endogenous SHG imaging of a wild type *C. elegans* nematode. The image was obtained from the anterior part of the worm. The sacromeres of the body wall muscles at the edges of the animal and the muscles of the chewing mechanism around the pharynx of the worm are clearly seen.

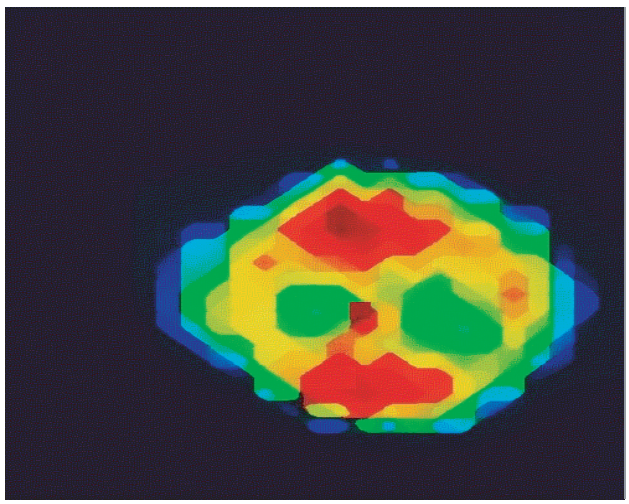

Figure 4. TPEF scanning image of a HL-60 cell, stained with merocyanine 540. The chromophore molecules have the potential to penetrate into the intracellular domain of the cell.

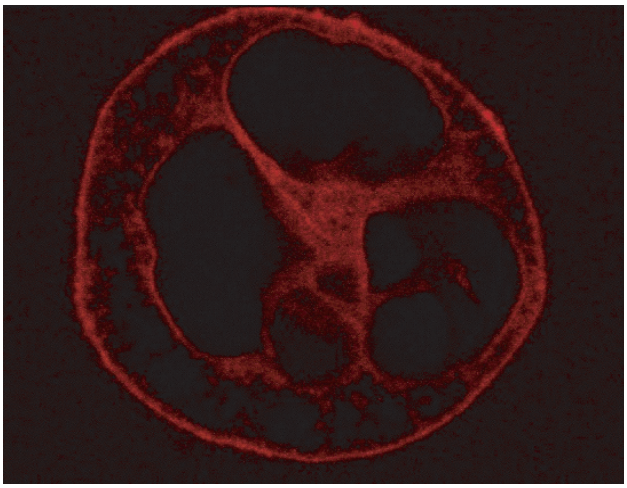

Figure 5. One-photon confocal fluorescence image of a HL-60 cell, stained with merocyanine 540. The characteristics of the confocal fluorescence image are the same as in the TPEF image shown in figure 4 (cell diameter $\sim$12 μm).

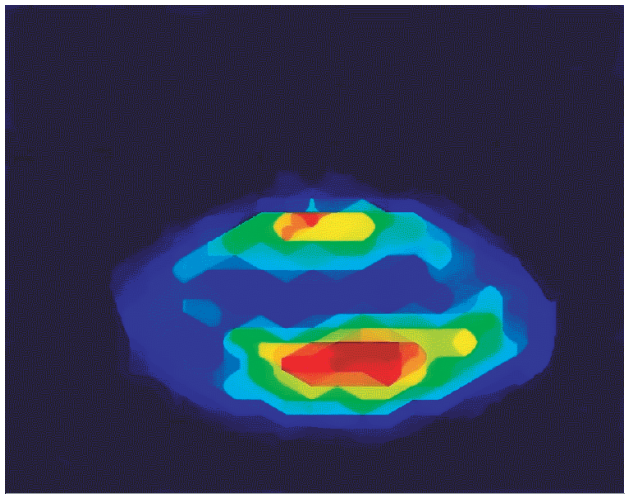

Figure 6. TPEF scanning image of a HL-60 cell, stained with PMF. The photosensitizer penetrates the cellular membrane and is localized inside the intracellular domain.

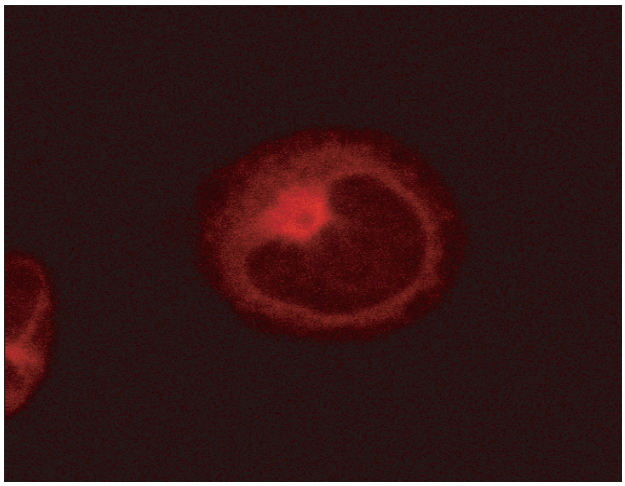

Figure 7. One-photon confocal fluorescence image of a HL-60 cell, stained with PMF. The characteristics of the confocal fluorescence image are similar to those the TPEF image depicted in figure 6 (cell diameter $\sim$10 μm).

fluorescence microscope was performed, and the results were similar (figure 5). For performing the one-photon measurements, the commercial confocal Radiance 2100 system from Bio-Rad was employed.

Apart from the TPEF imaging of the HL-60 cells stained with merocyanine 540, SHG imaging was tried, but not achieved. The hypothesis for this study was the known ability of merocyanine to generate SHG when its molecules have a global orientation [30, 31]. The failure of the SHG imaging forced us to consider two possible explanations: first, the photosensitizer penetrates the cellular membrane (as TPEF imaging indicates as well), thus having a small concentration of molecules bound on the membrane. Due to the small concentration, the SHG signal, produced by the merocyanine 540 molecules, is not detectable. Second, it is very likely that the molecules that remain bound to the cellular membrane lack a global orientation, and therefore their SHG signal is negligible and not detectable. These data (TPEF and SHG measurements) provide substantial evidence that MC-540 localizes in the intracellular domain of the HL-60 cell line. By using MC-540 as the photosensitizer, the main mechanism for cell apoptotic death during PDT is photodamage of sub-cellular organelles (e.g. mitochondria).

Furthermore, TPEF scanning images from the HL-60 cell line, stained with *Hypericum perforatum* L. extracts, were obtained. ME and the PMF were used as photosensitizers. These extracts have been recently used as photosensitizers during PDT against T24, NBT-II tumour bladder cells, yielding very promising results [32]. The main advantages of these extracts, in comparison with the commercial hypericin, are their low cost, extensive availability, adequate solubility, minimal toxicity and their use with a range of wavelengths. Our target is investigation of the sub-cellular localization of these new photosensitizers in the HL-60 cell line and elucidation of the possible mechanisms for cell killing during PDT.

Figure 6 shows a TPEF image of HL-60 cells stained with the PMF. A Nikon (50×, NA 0.8) objective lens was used, and the TPEF signal was detected in the backward direction. The scanning was performed in a specific z position where the TPEF signal coming from the specimen was maximum. The dimensions of the scanned region are $25 \times 35\ \mu m^2$. The minimum step in each direction was 1 μm. The main chromophore of the extracts is hypericin. Figure 6 shows that hypericin has penetrated the cellular membrane of HL-60 and it can be localized in the intracellular domain. The same results were obtained by performing one-photon confocal fluorescence imaging of a similar cell (figure 7). The ME exhibits the same behaviour as PMF regarding the binding of hypericin in the HL-60 cell line (figures are not presented). From other studies [33] it is known that hypericin is not strictly membrane bound and has the efficiency to penetrate and bind in structures in the intracellular domain of the cell. The cellular distribution of hypericin appears to be influenced by the cell type. In addition, the photodynamic killing efficacy of hypericin, which can be directly correlated to the intracellular accumulation of the photosensitizer, is dependent

on the cell type [34]. Investigations using intact cells [35] have indicated that hypericin, although it is not strictly bound in mitochondria, can critically affect the functions of these organelles in a photodependent manner. Our results present that the novel, low-cost, *Hypericum perforatum* L. extracts, very promising for PDT, exhibit the same potential, like pure hypericin, to penetrate into the intracellular domain of the cell. These data support the hypothesis that the mitochondria are the primary cellular cites for the *Hypericum perforatum* L. extract's photodynamic action.

5. Conclusions

Non-linear microscopy is a new and very promising technique that provides useful and unique information in various fields of medicine and biology. In this study TPEF and SHG images from biological samples were obtained. A compact, reliable, inexpensive non-linear imaging system has been developed. We collected detailed images of the anterior part of the *C. elegans* body by recording SHG signals. Reliable and valuable information in real time concerning the anatomy of *C. elegans* were acquired. Identification of the endogenous structural proteins that are the main contributors for the observation of the high SHG signals was achieved.

The second target of this study concerns the photosensitizers used in PDT and specification of the locations where these photosensitizers are bound in the membrane or the cytoplasm of cancer cells. The precise localization of the different photosensitizers inside the cell, using an imaging technique, is thought to be critical for determining the mode of cell death after PDT. We used the HL-60 cell line. Merocyanine 540 and *Hypericum perforatum* L. extracts were the photosensitizers that we investigated by recording TPEF images. It was shown that all the photosensitizers are not strictly membrane bound and they have the potential to penetrate into the intracellular domain of the cell. Similar results were obtained by performing one-photon confocal fluorescence imaging of the same specimens. We focused our study on the *Hypericum perforatum* L. extracts (PMF and ME) since they are new, inexpensive, low-toxicity photosensitizers, yielding very promising results during PDT against cancer cells. The possible mechanisms of cell killing during PDT, by using these extracts as photosensitizers, have been elucidated.

Acknowledgments

This work was supported by the UV Laser Facility operating at FORTH under the European Commission 'Improving Human Research Potential' programme (HPRI-CT-2001-00139), by the Integrated Project 'Molecular Imaging' (LSHG-CT-2003-503259) and by the European Molecular Biology Organization. NT is an EMBO Young Investigator. We thank G Vasilakis for his valuable help during the early experiments.

References

[1] Meglinski I V, Bashkatov A N, Genina E A, Churmakov D Y and Tuchin V V 2002 Study of the possibility of increasing the probing depth by the method of reflection confocal microscopy upon immersion clearing of near-surface human skin layers *Quantum Electron.* **32** 875–82

[2] Tuchin V V 1998 Coherence-domain methods in tissue and cell optics *Laser Phys.* **8** 807–49

[3] Denk W, Strickler J H and Webb W W 1990 Two-photon laser scanning fluorescence microscopy *Science* **248** 73–6

[4] Bloembergen N 1965 *Nonlinear Optics* (Singapore: World Scientific)

[5] Moreaux L, Sandre O, Blanchard-Desce M and Mertz J 2000 Membrane imaging by simultaneous second-harmonic and two-photon microscopy *Opt. Lett.* **25** 320–2

[6] Yeh A T, Nassif N, Zoumi A and Tromberg B J 2002 Selective corneal imaging combined second-harmonic generation and two-photon excited fluorescence *Opt. Lett.* **27** 2082–4

[7] Zoumi A, Yeh A and Tromberg B J 2002 Imaging cells and extracellular matrix *in vivo* by using second-harmonic generation and two-photon excited fluorescence *Proc. Natl Acad. Sci. USA* **99** 11014–19

[8] Zipfel W R, Williams R M, Christie R, Nikitin A Y, Hyman B T and Webb W W 2003 Live tissue intrinsic emission microscopy using multiphoton-excited native fluorescence and second harmonic generation *Proc. Natl Acad. Sci. USA* **100** 7075–80

[9] Shen Y R 1989 Surface properties probed by second-harmonic and sum-frequency generation *Nature* **337** 519–25

[10] Huang Y, Lewis A and Lewis L M 1988 Non-linear optical properties of potential sensitive styryl dyes *Biophys. J.* **53** 665–70

[11] Bouevitch O, Lewis A, Ben-Oren I, Wuskell J and Loew L 1993 Probing membrane potential with nonlinear optics *Biophys. J.* **65** 672–9

[12] Peleg G, Lewis A, Linial M and Loew L M 1999 Nonlinear optical measurement of membrane potential around single molecules at selected cellular sites *Proc. Natl Acad. Sci. USA* **96** 6700–4

[13] Lewis A, Khatchatouriants A, Treinin M, Chen Z, Peleg G, Friedman N, Bouevitch O, Rothman Z, Loew L and Sheres M 1999 Second-harmonic generation of biological interfaces: probing the membrane protein bacteriorhodopsin and imaging membrane potential around GFP molecules at specific sites in neuronal cells of *C. elegans Chem. Phys.* **245** 133–44

[14] Campagnola P J and Loew L M 2003 Second-harmonic imaging microscopy for visualizing biomolecular arrays in cells, tissues and organisms *Nature Biotechnol.* **21** 1356–60

[15] Mohler W, Millard A C and Campagnola P J 2003 Second harmonic generation imaging of endogenous structural proteins *Methods* **29** 97–109

[16] Campagnola P J, Millard A C, Terasaki M, Hoppe P E, Malone C J and Mohler W A 2002 Three-dimensional high-resolution second-harmonic generation imaging of endogenous structural proteins in biological tissues *Biophys. J.* **81** 493–508

[17] Brown E, McKee T, di Tomaso E, Pluen A, Seed B, Boucher Y and Jain R K 2003 Dynamic imaging of collagen and its modulation in tumors *in vivo* using second-harmonic generation *Nature Med.* **9** 796–801

[18] Moreaux L, Pons T, Dambrin V, Blanchard-Desce M and Mertz J 2003 Electro-optic response of second-harmonic generation membrane potential sensors *Opt. Lett.* **28** 625–7

[19] Millard A C, Jin L, Lewis A and Loew L M 2003 Direct measurement of the voltage sensitivity of second-harmonic generation from a membrane dye in patch-clamped cells *Opt. Lett.* **28** 1221–3

[20] Khatchatouriants A, Lewis A, Rothman Z, Loew L and Treinin M 2000 GFP is a selective non-linear optical sensor of electrophysiological processes in *Caenorhabditis elegans Biophys. J.* **79** 2345–52

[21] Pons T, Moreaux L, Mongin O, Blanchard-Desce M and Mertz J 2003 Mechanisms of membrane potential sensing with second-harmonic generation microscopy *J. Biomed. Opt.* **8** 428–31

[22] Dombeck D A, Blanchard-Desce M and Webb W W 2004 Optical recording of action potentials with second-harmonic generation microscopy *J. Neurosci.* **24** 999–1003
[23] Sulston J E, Schierenberg E, White J G and Thomson J N 1983 The embryonic cell lineage of the nematode *Caenorhabditis elegans Dev. Biol.* **100** 64–119
[24] The *C. elegans* Sequencing Consortium 1998 Genome sequence of the nematode *C. elegans*: a platform for investigating biology *Science* **282** 2012–18
[25] Mello C C, Kramer J M, Stinchcomb D and Ambros V 1991 Efficient gene transfer in *C. elegans*: extrachromosomal maintenance and integration of transforming sequences *EMBO J.* **10** 3959–70
[26] White J G, Southgate E, Thomson J N and Brenner S 1996 The structure of the nervous system of *Caenorhabditis elegans R. Soc. Lond. B: Biol. Sci.* **314** 1–340
[27] Brenner S 1974 The genetics of *Caenorhabditis elegans Genetics* **77** 71–94
[28] Danilatou V, Lydaki E, Dimitriou H, Papazoglou T G and Kalmanti M 2000 Bone marrow purging by photodynamic treatment in children with acute leukemia. Cytoprotective action of Amifostine *Leukemia Res.* **24** 427–35
[29] Chen J Y, Cheung N H, Fung M C, Wen J M, Leung W N and Mak N K 2000 Subcellular localization of merocyanine 540 (MC540) and induction of apoptosis in murine myeloid leukemia cells *Photochem. Photobiol.* **72** 114–20
[30] Uesu Y, Nakai R, Kato N, Menoret C, Kiat J M, Itoh M, Narahashi M and Kyomen T 2003 SHG microscopic studies on low temperature phase transitions of $SrTi_{16}O_3$ and $SrTi_{18}O_3$ *Ferroelectrics* **285** 19–26
[31] Tsuboi K, Seki K, Ouchi Y, Fujita K and Kajikawa K 2003 Formation of merocyanine self-assembled monolayer and its nonlinear optical properties probed by second-harmonic generation and surface plasmon resonance *Japan. J. Appl. Phys.* **42** 607–13
[32] Nseyo U O, Kim A H, Nseyo U U, Stayropoulos N E and Skalkos D 2004 Photodynamic therapy (PDT) with *Hypericum perforatum* L. extract induced significant *in vitro* cytotoxicity of human bladder cancer cells *Proc. Am. Assoc. Cancer Res.* **45** 4319
[33] Miskovsky P, Sureau F, Chinsky L and Turpin P Y 1995 Subcellular distribution of hypericin in human cancer cells *Photochem. Photobiol.* **62** 546–9
[34] Vandenbogaerde A L, Cuveele J F, Proot P, Himpens B E, Merlevede W J and de Witte P A M 1997 Differential cytotoxic effects induced after photosensitization by hypericin *J. Photochem. Photobiol.* B **38** 136–42
[35] Miccoli L, Beurdeley-Thomas A, De Pinieux G, Sureau F, Oudard S, Dutrillaux B and Poupon M F 1998 Light-induced photoactivation of hypericin affects the energy metabolism of human glioma cells by inhibiting hexokinase bound to mitochondria *Cancer Res.* **58** 5777–86